Contents lists available at ScienceDirect

Marine Environmental Research

journal homepage: http://ees.elsevier.com

Effects of long-term exposure to reduced pH conditions on the shell and survival of an intertidal gastropod

Sofía Viotti, Carlos Sangil, Celso Agustín Hernández, José Carlos Hernández*

Departamento de Biología Animal, Edafología y Geología, Universidad de La Laguna, Canary Islands, Tenerife, Spain

ARTICLE INFO

Keywords
pH variability
Phorcus sauciatus
CO_2 vent
Gastropod
Atlantic ocean
Population dynamics

ABSTRACT

Volcanic CO_2 vents are useful environments for investigating the biological responses of marine organisms to changing ocean conditions (Ocean acidification, OA). Marine shelled molluscs are highly sensitive to changes in seawater carbonate chemistry. In this study, we investigated the effects of reduced pH on the intertidal gastropod, *Phorcus sauciatus*, in a volcanic CO_2 vent off La Palma Island (Canary Islands, North East Atlantic Ocean), a location with a natural pH gradient ranging from 7.0 to 8.2 over the tidal cycles. Density and size-frequency distribution, shell morphology, shell integrity, fracture resistance, and desiccation tolerance were evaluated between populations from control and CO_2 vent sites. We found no effects of reduced pH on population parameters or desiccation tolerance across the pH gradient, but significant differences in shell morphology, shell integrity, and fracture resistance were detected. Individuals from the CO_2 vent site exhibited a higher shell aspect ratio, greater percentages of shell dissolution and break, and compromised shell strength than those from the control site. Our results highlight that long-term exposure to high pCO_2 can negatively affect the shell features of *P. sauciatus* but may not have a significant effect on population performance. Moreover, we suggest that loss of shell properties could lead to changes in predator-prey interactions.

1. Introduction

Anthropogenic emissions of carbon dioxide (CO_2) are causing modifications of the inorganic carbon chemistry of the ocean, leading to ocean acidification (OA). This process is characterized by reductions in seawater pH, carbonate ion [CO_3^{2-}] concentrations and decreased aragonite and calcite saturation states (Ω) (IPCC et al., 2014). Several studies have reported that calcified marine invertebrates exhibit varying biological responses to OA (Harvey et al., 2013; Kroeker et al., 2013). Shelled molluscs, which play key ecological roles in the marine ecosystem (Gazeau et al., 2013), are particularly vulnerable to alterations in seawater carbonate chemistry (Duquette et al., 2017). Reductions in pH have a direct impact on the metabolism of gastropods and bivalves and can affect their internal pH homeostasis (Pörtner, 2008) and key physiological processes, such as larval development (Gaylord et al., 2011), shell formation (Onitsuka et al., 2014), and reproduction (Harvey et al., 2016).

Changes in CO_3^{2-} concentrations can impair shell biomineralization processes and alter shell composition in molluscs (Langer et al., 2018). Previous studies have shown that certain species of gastropods exposed to elevated CO_2 partial pressure (pCO_2) levels experienced reductions in net calcification and shell mechanical properties, while others showed neutral or even positive responses (Ries et al., 2009; Rodolfo-Metalpa et al., 2011; Duquette et al., 2017). The variability in responses suggests that calcium carbonate ($CaCO_3$) production depends on the ability of each species to build and maintain protective shells under lower pH values and CO_3^{2-} concentrations (Findlay et al., 2011). However, the physiological costs of maintaining metabolic rates and coping with external shell dissolution across pH gradients (McClintock et al., 2009; Nienhuis et al., 2010; Harvey et al., 2016) can lead to reductions in shell growth, strength, and changes in shell morphology (Melatunan et al., 2013; Coleman et al., 2014; Rühl et al., 2017; Meng et al., 2018).

Previous evidence suggests that changes in the calcified structure of marine gastropods could pose a threat to their capacity to cope with environmental stressors, such as wave action, thermal stress at low tide, and predation (Vermeij, 1973; Garrity, 1984; Kroeker et al., 2014), which could trigger changes at the population level (Kurihara, 2008). Recent research at CO_2 vents in the Mediterranean has shown a significant reduction in the abundance (Hall-Spencer et al., 2008; Kroeker et al., 2011) and proportion of gastropod females (Harvey et al., 2016) exposed to elevated pCO_2 levels. Furthermore, changes in shell shape, size, and thickness in response to changes in carbonate

* Corresponding author.
E-mail address: jocarher@ull.es (J.C. Hernández)

https://doi.org/10.1016/j.marenvres.2019.104789
Received 14 April 2019; Received in revised form 7 September 2019; Accepted 7 September 2019
Available online xxx
0141-1136/

chemistry have been observed in limpets, whelks, top-shells, and nassariid snails living near CO_2 vents (Garilli et al., 2015; Duquette et al., 2017). Similar effects on the shell, including progressive shell dissolution and deterioration, have been detected in dove and triton snail populations in vent environments in Taiwan (Chen et al., 2015) and Japan (Harvey et al., 2018).

Although mesocosm laboratory experiments have provided relevant information about the vulnerability of gastropods to changes in seawater chemistry, natural acidified systems present certain advantages when investigating the effects of long-term exposure to pCO_2 gradients on intertidal communities (Agostini et al., 2018; Milazzo et al., 2019). These natural laboratories allow the incorporation of multiple environmental drivers and ecosystem processes (such as carbonate system parameters, food availability, predation, etc.) (González-Delgado and Hernández, 2018). However, the use of CO_2 seeps for OA studies also presents certain challenges. Pronounced fluctuations in venting intensity, pH oscillations due to coastal dynamics (such as photosynthesis, tides, upwelling events), and interacting gradients in carbonate chemistry may confound the effects of high pCO_2 on organisms (Rastrick et al., 2018). In addition, larval dispersal strategies and connectivity among populations may also be potential challenges when assessing the resilience of species to high pCO_2 environments (Sunday et al., 2014).

The present study estimated the effects of long-term exposure to reduced pH conditions on the intertidal gastropod *Phorcus sauciatus* (Koch, 1845) at a volcanic CO_2 vent on La Palma Island (Canary Islands). This vent system creates natural pCO_2 and pH gradients along the shoreline with the lowest pH occurring during low tide (≤7.5) (Hernández et al., 2017). *P. sauciatus* is a mid-littoral species found on the rocky shores of the north-eastern Atlantic Ocean (Donald et al., 2012; Uribe et al., 2017). In the Canary Archipelago, this species is relatively abundant along the cobble beaches and volcanic platforms, and it is also a local fisheries resource (Alfonso et al., 2015). In order to investigate the effects of pH fluctuation on the *P. sauciatus* population, comparative studies of size-frequency distribution and density were conducted between vent, transition, and control populations. Furthermore, to assess whether long-term exposure to high pCO_2 alters the development and functions of the shell, we evaluated several parameters: (1) shell morphology; (2) shell integrity (percentages of corrosion and break); and (3) fracture resistance across the natural pCO_2 gradient. Finally, we investigated whether reduced pH conditions had an influence on desiccation tolerance of individuals.

2. Methods

2.1. Study areas and carbonate system parameters

Three sampling areas were selected in order to define the study sites. Two sampling areas were situated on the coast of Fuencaliente (La Palma Island, Canary Islands, 28º27′N-17º50′W) (Fig. 1), a point at which a shallow-water CO_2 vent is located (Hernández et al., 2017). The volcanic activity in La Palma took place exclusively on the southern part of the island, the point at which Cumbre Vieja basaltic complex is located (Carracedo et al., 2001). Numerous eruptive centers that extend from the North-South rift zone of Cumbre Vieja to the southern coast of the island have been recently detected (Padrón et al., 2015). We also selected one control location situated in Punta Hidalgo (TI) (Fig. 1) in which no volcanic activity and CO_2 seepage were observed in order to avoid sampling populations affected by acidic waters at any time. All three study areas presented the same wave exposure and type of habitat, consisting of a mix of bare basaltic rocky beach and boulder fields (<1 m in diameter) with a medium slope (≈45° inclination) without any well-developed macroalgae communities.

Seawater chemistry data were collected in April 2017. The pCO_2 concentration and pH were recorded for each study area. The pCO_2 concentration was recorded using an *in situ* C-sense pCO_2 sensor (Turner Designs) with a measurement range of 4000 ppm. The pH was recorded using an *in situ* SBE 18 pH sensor (Seabird Electronics), previously calibrated using a three-point calibration program against precision National Institute of Standards and Technology (NIST) buffer solution (pH 4, 7, and 10 ± 0.02). The sensor systems were powered by a 12V battery and connected to a data logger. The sensors recorded pCO_2 concentration and pH every minute over a 24 h period at < 5 m depth. These measurements were obtained for two days.

Additionally, three replicated water samples were taken at two depth levels: (1) sea surface and (2) bottom (<5 m) and stored in hermetically sealed borosilicate bottles. Total seawater alkalinity (T_A) measurements from each replicate bottle took place half an hour after sampling to avoid sample contamination. T_A was measured according to Dickson's method (Dickson et al., 2007) using an open cell potentiometric titrator (MetrohmDosimat665) and 0.01 N HCl with a salinity of 35 ppm for the titration of the samples. Discrete salinity and temperature measurements were taken using a hand-held conductivity meter (Hannah Instruments HI98192). Triplicate salinity and temperature records were taken during low and high tides.

pCO_2 values that exceeded the detection limit of the C-sense pCO_2 sensor (4000 ppm) and the rest of carbonate chemistry parameters were calculated from the resulting dataset (pH, T_A, salinity and temperature measurements) using CO_2SYS software (Lewis and Wallace, 1998). Calculations were based on GEOSEC constants with K1 and K2 from Mehrbach et al. (1973), $KHSO_4$ from Dickson (1990), and [B]T values from Uppström (1974).

2.2. Population parameters (size and population density) and collection

Sampling was performed along the mid-littoral zone of the rocky shore according to the classic zonation schemes (Stephenson and Stephenson, 1949). At each study area, sampling was conducted using four 10 × 2 m transecting lines running parallel to the shore. Shell length (distance from the shell apex to the base) and maximum shell width (major diameter of the body whorl) of individuals from each transect were measured using a digital calliper (precision: ± 0.01 mm). A total of 949 *P. sauciatus* individuals (control: $n = 213$; transition: $n = 408$; vent: $n = 328$) were measured.

Population density (number of individuals * m^{-2}) was calculated from the resulting data set in each transect. The population structure was defined by a size-frequency distribution diagram, obtained maximum shell width classification. Individuals were grouped into 10 size classes with 2 mm intervals each. Samples of *P. sauciatus* from the three study areas (N = 405; $n = 135$ *per* study site) were collected and placed inside portable refrigerators filled with seawater. All collected individuals were transported to the laboratory within 24 h from the actual collection time for further experimental treatment (shell condition, fracture resistance, and desiccation tolerance).

2.3. Shell morphology and condition (corrosion and break)

All shell length and width data from each sampling site (N = 949; control: n = 213; transition: n = 408; vent: n = 328) were used for calculations of shell aspect ratio (shell length:shell width). Mean shell aspect ratios were used for comparisons of shell morphology between populations of each study area.

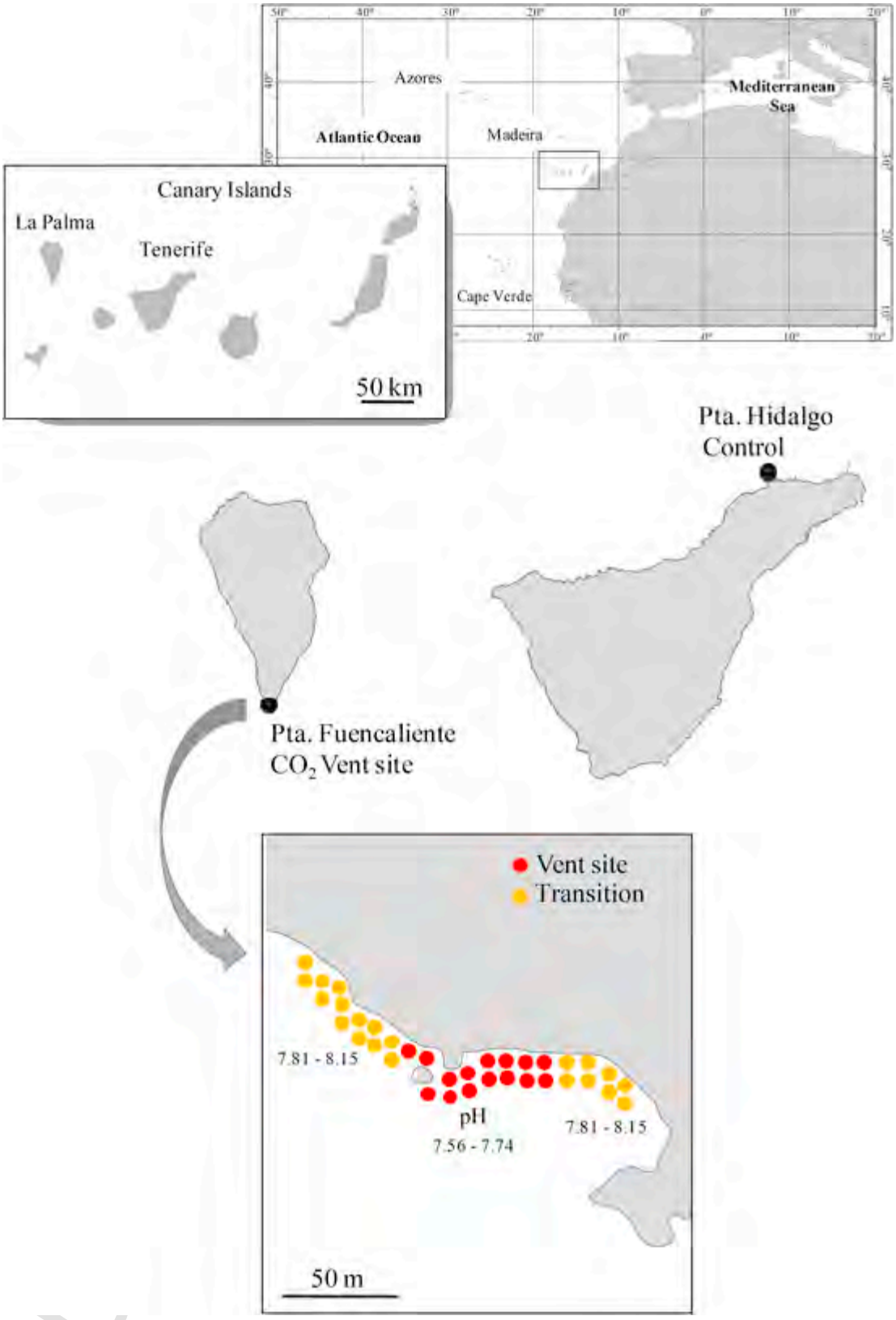

Fig. 1. Maps of the study areas at Punta del Hidalgo, Tenerife (Control) and Fuencaliente, La Palma (transition and vent site). The dots represent the pH range of each study area.

Shell condition was evaluated by calculating the percentages of corrosion and break in the shell of 99 individuals ($n = 33$ *per* study site) randomly selected from the available samples previously collected at the study areas. Shell with <15 mm of width (major diameter of the body whorl) were removed from consideration and replaced by another individual. Shell corrosion was defined as the area of the shell surface with visible signs of dissolution, while shell break was defined as the

area with presence of holes or apex truncation. Natural fractures due to mechanical stress were excluded. All individuals, previously fixed in 70% ethanol, were photographed with a digital camera with a high-resolution macro lens maintaining consistent capture conditions. Two photographs *per* individual were taken: (1) one in an apical view and (2) another in a basal view. For measurements of shell condition, total shell, corrosion, and break areas were measured in each photograph using ImageJ 1.51n software (Schneider et al., 2012). A total of 198 images were analysed. The percentages of corrosion and break in the shell were calculated for each population.

2.4. Fracture resistance

Shell fracture resistance was tested in 180 individuals ($n = 60$ *per* study site) of shell width (major diameter of the body whorl) ranging from 10 to 24 mm (small: <14 mm; medium: 14–18 mm; large: > 18 mm) to facilitate comparison between different sizes. Fracture resistance was measured as the maximum force (kilogram force, kgF) that the shell could tolerate before breaking. Mechanical tests were conducted using a 7t digital compression testing machine (Model MUE-1E, Salmer-Pacam) with a load cell fitted to the precise control over the force application. All individuals were previously fixed in 70% ethanol, and shell width was measured using a digital calliper (precision: ± 0.01 mm). Fracture resistance was examined individually at a constant speed of 1.5 mm * min^{-1}. The force was applied perpendicular to the axis of coiling to ensure stability during compression, and representative measurements of the force exerted by predators on the shell were obtained (Cotton et al., 2004).

2.5. Desiccation tolerance

Desiccation tolerance was tested in a total of 225 individuals of similar size (shell width ranging between 15 and 17 mm) collected at each sampling area ($n = 75$ *per* study site). Individuals were exposed to three temperature treatments of 20, 30, and 40 °C. We only selected individuals of similar shell width in order to facilitate comparison between populations. Laboratory experiments began within 48 h from the time of collection of individuals. Groups of 75 individuals ($n = 25$ *per* study site) were placed on porcelain crucibles and exposed to each temperature treatment during a five-day cycle. Heat stress conditions experienced by intertidal organisms during emersion periods at low tide (Garrity, 1984) were simulated using a programmable convection oven (Heraeus UT12, Heraeus Instruments). In order to imitate the semidiurnal tidal regime that occurs in the Atlantic, heat stress trials ran for a period of 5 h *per* day. Individuals used for all temperature treatments were maintained in three aquaria filled with filtered seawater (ambient temperature 17 °C, salinity 36 ppm) and constant aeration with an air pump. Groups of each population were marked with a colored dot on the shell using indelible and non-toxic paint. After each trial, individuals were returned to the aquariums and the treatment was repeated 24 h later using the same individuals. The temperature was held steady and the individuals who died during each trial were not replaced. The mortality of individuals was calculated throughout the hours of treatment at each temperature cycle applied.

2.6. Statistical analyses

Differences in size-frequency distributions between populations were tested using a Pearson's chi-squared test (χ^2) with R 3.3.1 software (R Development Core Team, 2016).

The remaining data were analysed using permutation tests for univariate analysis of variance (PERANOVA). The population density and the percentage of corrosion and break in the shell between sites were compared separately by one-way PERANOVA tests with site as the fixed factor (three levels [control, transition; and vent]). Differences in shell aspect ratio (shell length:shell width) between populations were tested using a two-way PERANOVA test with site treated as the fixed factor (three levels [control, transition, and vent) and transect as a random factor, nested in site (four levels consisting of transects 1–4).

In order to evaluate the effects of pH fluctuation on fracture resistance, a two-way PERANOVA test was applied with site (three levels [control, transition, and vent]) and size (three levels [1small, medium, and large]) as fixed factors. Additionally, the linear regression used for the variables examined force and shell width was carried out using StatPlus Mac OS software (AnalystSoft Inc., 2013). Desiccation tolerance of individuals was analysed using a three-way PERANOVA test with site (three levels [control, transition, and vent]), temperature (three levels [20, 30, and 40 °C]) and hours of emersion (five levels ranging from 5 to 25 h in 5 h increments) as fixed factors.

Statistical analyses were carried out using PRIMER 6 & PERMANOVA v.1.0.1 software (Anderson et al., 2008). Significant differences were examined using *a posteriori* pairwise comparisons by permutations (Anderson, 2001). For all tests, 4999 permutations were undertaken on Euclidean distance matrices and $p < 0.05$ was considered significant.

3. Results

3.1. Seawater carbonate chemistry at study sites

According to the carbonate system results at each sampling site, we defined three study areas characterized by variations in carbonate chemistry parameters: (1) control site; (2) transition site; and (3) vent site (Table 1). At the control site, these parameters (pH, pCO_2, T_A, Ω calcite, and Ω aragonite saturation states) remained relatively stable between tide periods but showed increasing fluctuations at the transition and vent sites with, for example, lower pH levels (Table 1). During low tide, the pCO_2 concentration increased significantly at the transition and vent sites with a reduction in pH to 7.6 and 7.0 units, respectively. In contrast, the pH reached values > 8.0 units during high tide (Fig. 2, Table 1). Calcite and aragonite saturation states also showed fluctuations between tide periods and presented significant reductions by the CO_2 vent during low tide at both transition and vent sites. The lowest values were measured at the vent site (Ω calcite = 1.74 ± 0.05 and Ω aragonite = 1.20 ± 0.03), reaching reduced values of Ω calcite = 0.56 and Ω aragonite = 0.39 (Table 1). Changes in T_A were evident at the transition and vent sites. Greater fluctuations in T_A over tidal cycles were detected at the vent site. On average, T_A was higher during low tide (mean = 3088.44 mmol/kgSW) than at the transition site (mean = 2804.45 mmol/kgSW) (Table 1). No differences in salinity were detected. Seawater temperature remained relatively constant among sites, with mean temperature ranged between 20.8 °C and 23.6 °C (Table 1).

3.2. Population parameters (size and population density)

Population density did not differ significantly between control and transition and vent sites (Pseudo-$F = 1.233$, $p = 0.34$). Mean ± SE densities are presented in Fig. 3. Size-frequency distributions did not differ significantly among sites (chi-squared test, $\chi^2 = 55.134$, df = 16, $p < 0.001$). Populations were structured around one size class and showed a unimodal distribution with individual sizes ranging from 6 to 23 mm at all three study sites (Fig. 4). At the control site, 17 mm was most frequent size, while at transition and vent sites, it was 15 mm (Fig. 4).

Table 1
Carbon System parameters (mean ± SE) during low and high tide collected at each study site. S = discrete salinity, T = temperature ºC, T_A = total alkalinity (mmol/kgSW), $\Omega_{calcite}$ = calcite saturation, $\Omega_{aragonite}$ = aragonite saturation. * = Seawater carbonate chemistry calculated using the data collected with the probe; a, b = mean pH and temperature calculated from 10 data collected with the sensors; c = Average total alkalinity calculated from day 1 and 2.

Site	Day	S	T	Low Tide				S	T	High Tide			
				pH	T_A	$\Omega_{calcite}$	$\Omega_{aragonite}$			pH	T_A	$\Omega_{calcite}$	$\Omega_{aragonite}$
Control	1	36.0	21.5	8.14	2598.25	4.48	3.09	36.0	20.9	8.11	2583.30	4.21	2.90
	2	36.1	21.6	8.04 ± 0.01	2607.26 ± 12	3.72 ± 0.07	2.57 ± 0.05	36.1	21.1	8.16 ± 0.01	2508.10 ± 6	4.49 ± 0.10	3.10 ± 0.08
	*	36.0	23.67[a]	8.1[b]	2602.76[c]	5.46	3.77	36.0	23.53[a]	8.18[b]	2545.7[c]	5.04	3.48
Transition	1	36.0	21.4	7.95 ± 0.09	2798.68 ± 69	3.34 ± 0.51	2.31 ± 0.36	36.0	21.1	8.08 ± 0.01	2626.33 ± 7	4.04 ± 0.09	2.79 ± 0.06
	2	36.1	21.7	7.81 ± 0.01	2810.21 ± 11	2.53 ± 0.05	1.74 ± 0.03	36.1	20.8	8.15 ± 0.01	2524.96 ± 8	4.44 ± 0.08	3.06 ± 0.06
	*	36.1	22.6[a]	7.7[b]	2804.45[c]	2.10	1.45	36.1	22.54[a]	8.1[b]	2575.65[c]	4.3	2.97
Vent	1	36.0	21.4	7.56 ± 0.02	3287.03 ± 41	1.74 ± 0.05	1.20 ± 0.03	36.0	21.0	7.95 ± 0.07	2754.53 ± 11	3.29 ± 0.44	2.27 ± 0.45
	2	36.1	21.6	7.74 ± 0.02	2889.84 ± 7	2.25 ± 0.10	1.55 ± 0.08	36.1	20.8	8.14 ± 0.01	2526.11 ± 10	4.36 ± 0.09	3.01 ± 0.06
	*	36.1	22.99[a]	7.05[b]	3088.44[c]	0.56	0.39	36.1	22.39[a]	8.18[b]	2640.32[c]	5.10	3.52

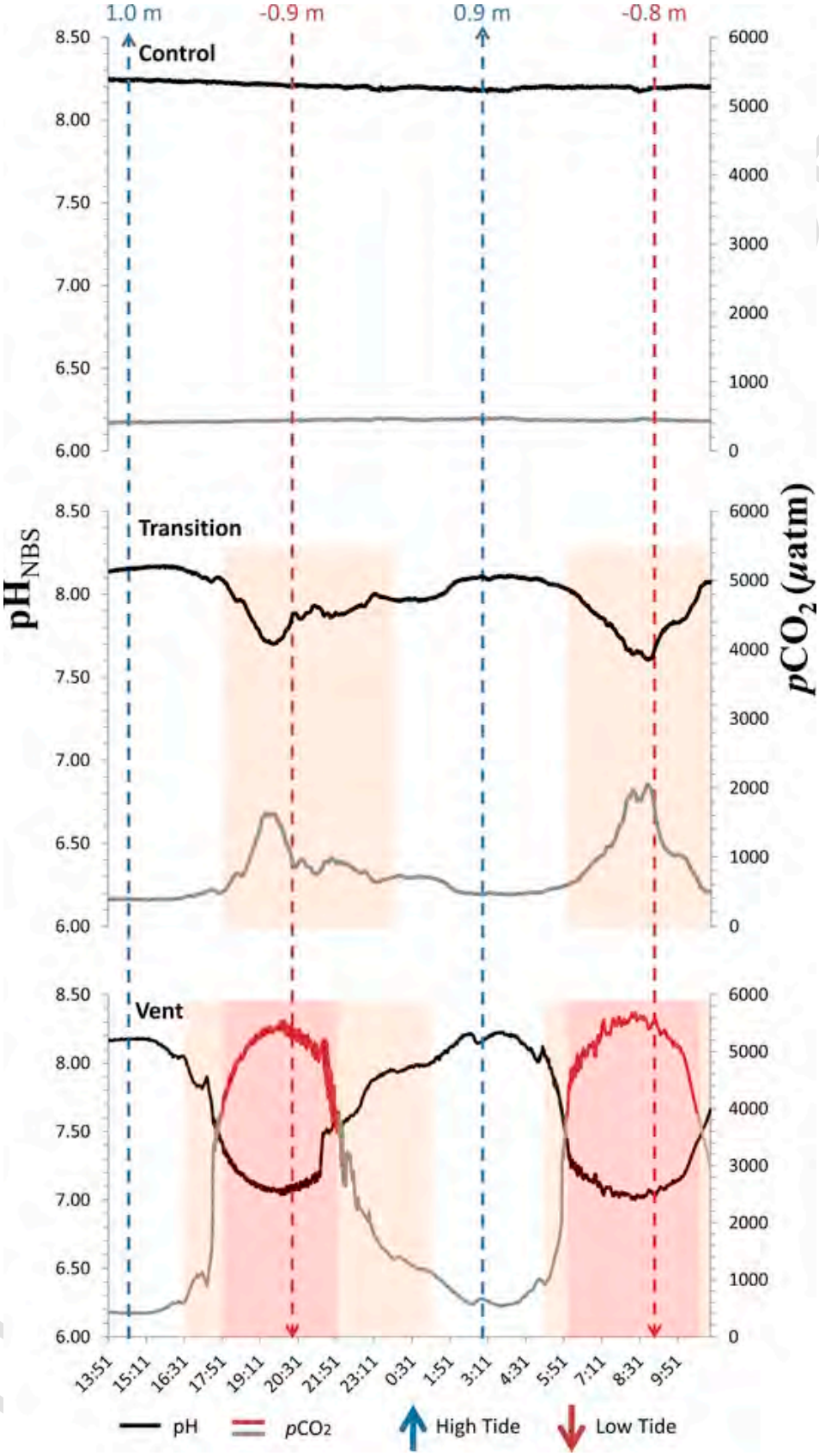

Fig. 2. Seawater pH_{NBS} and pCO_2 (µatm) fluctuation in the study sites: (1) control; (2) transition; and (3) vent. Twenty-four hour study using underwater sensors with continuous data collection. Tidal heights on the top of the graph use mean sea level as reference and were taken from the tide tables for Santa Cruz de La Palma. Red shade area delineate the hours of

the day with pHs <7.5; and orange shaded areas delineate the hours of the day with pH values between 8.0 and 7.5. (For interpretation of the references to color in this figure legend, the reader is referred to the Web version of this article.)

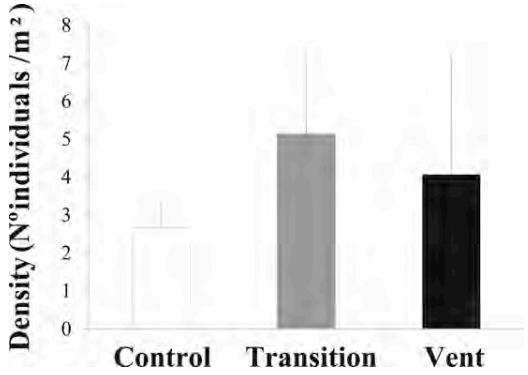

Fig. 3. Density (number of individuals/m^2) of *Phorcus sauciatus* (mean ± SE) recorded at each study: (1) control; (2) transition; and (3) vent.

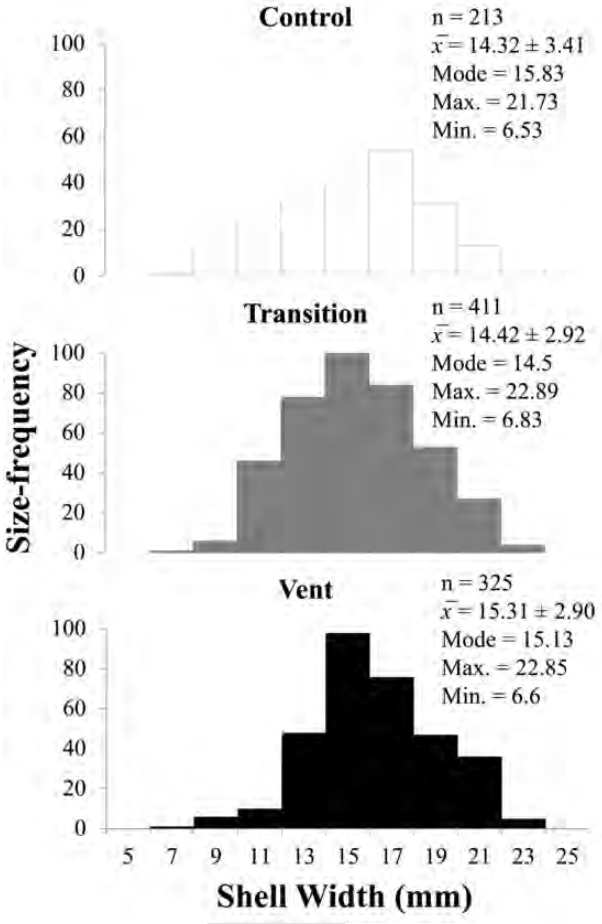

Fig. 4. Size-frequency distributions of *P. sauciatus* at each study site: (1) control; (2) transition; and (3) vent and descriptive statistical analyses (n = number of individuals, б = mean ± SE).

3.3. Shell morphology and condition (corrosion and break)

Shell aspect ratio differed significantly between study sites (Pseudo-F = 5.669, p = 0.014). An *a posteriori* pairwise test showed that the shell aspect ratio only differed significantly between the control and vent sites (Pairwise test, t = 3.636, p = 0.0044) (Table 2). Individuals from the control site exhibited a lower shell aspect ratio (mean = 0.53 ± 0.06) compared to individuals from the vent site (mean = 0.56 ± 0.06) (Fig. 5). On average, shells from the vent site were relatively taller (mean shell length = 8.64 ± 2.01) and wider (mean shell width = 15.31 ± 2.89) than those at the control site (mean shell length = 7.72 ± 2.29; mean shell width = 14.32 ± 3.41).

Table 2
Results of the two-way permutational ANOVA analyzing shell aspect ratio (shell length: shell width) with site (fixed factor; three levels: control, transition, vent) and transect (random factor nested in site; four levels: transect 1, transect 2, transect 3, transect 4). Results of *a posteriori* pairwise analysis for the levels of the factor site ($p < 0.05$).

Shell aspect ratio				
Source of variation	*df*	MS	Pseudo-F	*p* (perm)
Site	2	6.9919E-2	5.6691	0.014
Transect (Site)	9	1.3855E-2	3.6892	0.0006
Residual	937	3.7554E-3		
Total	948			
Pairwise analyses				
Site	*t*		*p* (perm)	
Control *vs* Vent	3.6368		0.0044	
Control *vs* Transition	1.4702		0.1778	
Transition *vs* Vent	2.0818		0.0534	

The percentages of shell corrosion and break differed significantly in both cases (% corrosion: Pseudo-F = 194.2, p = 0.0002; % break: Pseudo-F = 8.314, p = 0.001), among the three sites (Table 3). *A posteriori* pairwise tests showed that these percentages at the control site differed significantly from those at the transition (Pairwise test, % corrosion: t = 20.147, p = 0.0002; % break: t = 4.206, p = 0.0002) and vent sites (Pairwise test, % corrosion: t = 18.273, p = 0.0002; % break: t = 3.813, p = 0.0002). In contrast, shell corrosion and break did not differ significantly between the transition and vent sites (Pairwise test, % corrosion: p = 0.582; % break: p = 0.281).

On average, shells from the transition and vent site exhibited higher and similar percentages of shell corrosion (transition = 37.63 ± 9.26; vent = 39.01 ± 10.81) and break (transition = 1.89 ± 2.56; vent = 2.86 ± 4.29) than those at the control site (% corrosion = 2.67 ± 3.7; % break = 0.02 ± 0.03) (Fig. 6).

3.4. Fracture resistance

Fracture resistance differed significantly between study sites and shell sizes (small (S): <14 mm; medium; (M): 14–18 mm; large (L): >18 mm) (Pseudo-F = 4.022, p = 0.0028). An *a posteriori* pairwise test for the interaction between these two factors showed that fracture re-

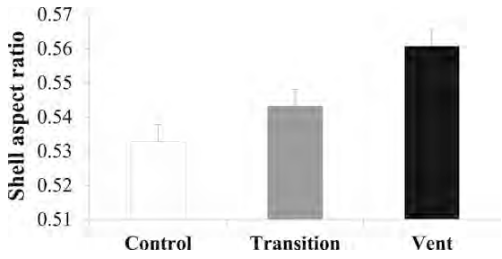

Fig. 5. Aspect ratio (mean ± SE) between shell length (mm) and width (mm) of *P. sauciatus* recorded at each study site (control, transition, and vent).

Table 3
Results of the one-way permutational ANOVA analyzing (A) the percentage of corrosion and (B) the percentage of break between sites (fixed factor; three levels: control, transition, vent). Results of *a posteriori* pairwise analyses analysis for the levels of the factor site ($p < 0.05$).

A. Percentage of corrosion				
Source of variation	*df*	MS	Pseudo-F	*p* (perm)
Site	2	13999	194.2	0.0002
Res	96	72.083		
Total	98			
Pairwise analyses				
Site	*t*		*p* (perm)	
Control *vs* Vent	18.273		0.0002	
Control *vs* Transition	20.147		0.0002	
Transition *vs* Vent	0.55758		0.582	
B. Percentage of break				
Source of variation	*df*	MS	Pseudo-F	*p* (perm)
Site	2	69.173	8.3148	0.001
Res	96	8.3192		
Total	98	936.99		
Pairwise analyses				
Site	*t*		*p* (perm)	
Control *vs* Vent	3.8139		0.0002	
Control *vs* Transition	4.2065		0.0002	
Transition *vs* Vent	1.1211		0.281	

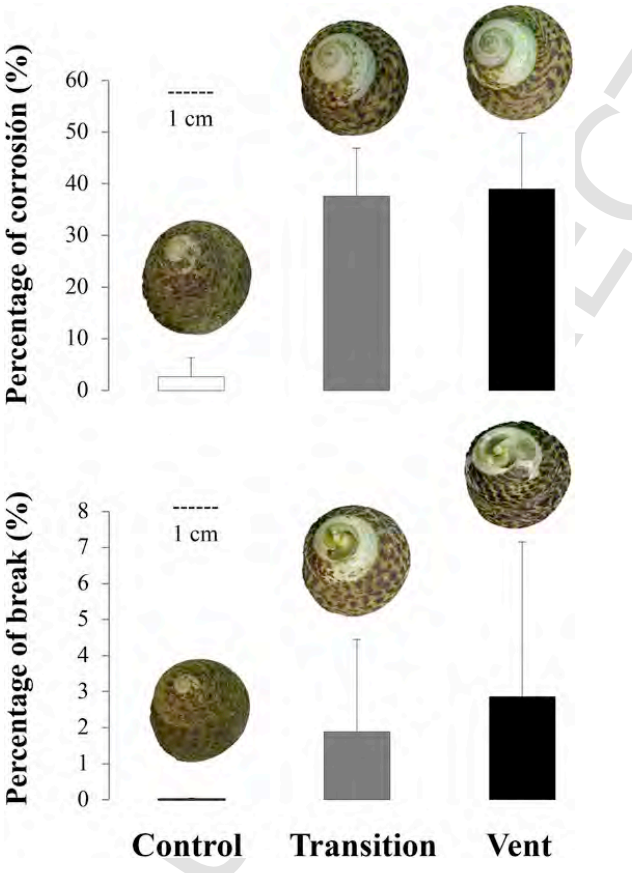

Fig. 6. Percentages of shell corrosion and break (mean ± SE) at each study site: (1) control; (2) transition; and (3) vent. Digital photographs of representative individuals collected at the study sites (Scale bars = 1 cm).

sistance differed significantly between all shell sizes at the control site (Pairwise test, S-M: $t = 4.132$, $p = 0.0006$; S-L: $t = 6.909$, $p = 0.0002$; M-L: $t = 3.153$; $p = 0.0036$). At the transition site, the fracture resistance of small and medium-sized shells differed significantly when compared to the large-sized shells (Pairwise test, S-L: $t = 4.65$; $p = 0.0002$; M-L: $t = 4.067$; $p = 0.0002$), but did not between each other (Pairwise test, S-M: $p = 0.3154$). In contrast, the fracture resistance did not differ significantly between any of the shell sizes at the vent site (Pairwise test, S-M: $p = 0.7206$; S-L: $p = 0.093$; M-L: $p = 0.0682$) (Table 4).

Linear regression curves showed a significant relationship between the force and shell width variables at the control and transition sites; however, no correlation between these variables was obtained for the vent site (Fig. 7). Specifically, the mean force needed to fracture the shells from the control site increased with shell width (Mean KgF: S = 13.05 ± 2.93; M = 17.8 ± 4.23; L = 22.70 ± 5.52). In contrast, small and medium-sized shells from the transition site fractured with similar force ranges (Mean KgF: S = 17.10 ± 4.39; M = 18.60 ± 4.74) and on average, were less resistant than large-sized shells (Mean KgF: L = 30 ± 11.60). Similarly, shells from the vent site fractured in similar force ranges regardless of size (Mean KgF: S = 19.70 ± 5.08; M = 18.90 ± 7.03; L = 23.03 ± 6.74) (Fig. 7).

3.5. Desiccation tolerance

Desiccation tolerance did not differ significantly between study sites (Pseudo-$F = 1.297$, $p = 0.0002$), but differed significantly between temperature and hours of emersion (Pseudo-$F = 25.619$, $p = 0.1872$) (Table 5). An *a posteriori* pairwise test for the interaction between these two factors showed that desiccation tolerance differed significantly between the hours of emersion at 30 and 40 °C but did not differ among any of the emersion hours at 20 °C. Particularly, significant differences were observed between 10 h and 5, 15, 20, 25 h emersion, and between 15 and 20 h emersion at 30 °C. At 40 °C significant differences were observed between almost all of the emersion hours but not between 15 and 20 h or 20 and 25 h of emersion (Table 5).

No mortality was observed during any of the emersion hours at 20 °C ($n = 0$) (Fig. 8). In contrast, mortality occurred within the first

Table 4
Results of the two-ways permutational ANOVA analyzing shell crushing resistance with site (three levels: control, transition, vent) and size (three levels: small: <14 mm; medium: 14–18 mm, large: >18 mm) as fixed factors. Results of *a posteriori* pairwise analysis for the interaction of factors site and size ($p < 0.05$).

Fracture resistance						
Source of variation	*df*		MS	Pseudo-F	*p* (perm)	
Site	2		254.93	6.4829	0.0022	
Size	2		1240.4	31.545	0.0002	
Site x Size	4		158.16	4.022	0.0028	
Res	171		39.323			
Total	179					
Pairwise analyses						
Size	Control		Transition		Vent	
	t	*p*	*t*	*p*	*t*	*p*
Small *vs* Medium	4.1321	0.0006	1.0386	0.3154	0.4124	0.7206
Small *vs* Large	6.9098	0.0002	4.6506	0.0002	1.7618	0.093
Medium *vs* Large	3.1536	0.0036	4.0676	0.0002	1.8937	0.0682

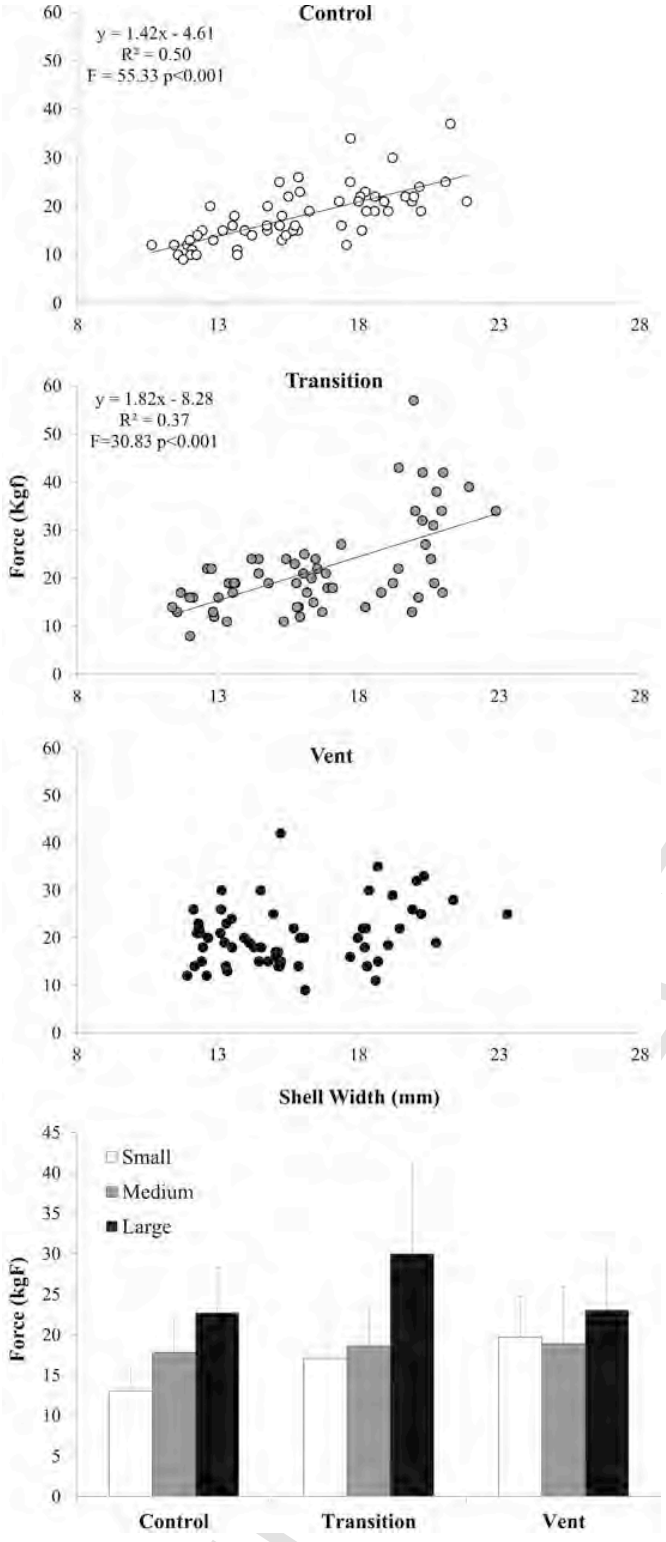

Fig. 7. A. Relationship between forces applied (kgF) and shell width (mm) for *P. sauciatus* individuals from each study site: (1) control; (2) transition; and (3) vent. B. Force applied (kgF) (mean ± SE) to achieve the fracture in shells (small: < 14 mm; medium: 14–18 mm, and large: > 18 mm) of individuals from each study site (control, transition, and vent).

5 h of exposure at 30 °C (control: $n = 0$; transition: $n = 2$; vent: $n = 2$) and increased until 15 h of treatment (control: $n = 3$; transition: $n = 12$; vent: $n = 10$). Except for one individual, no mortality was observed within the following emersion hours (25 h, control: $n = 3$; transition: $n = 12$; vent: $n = 11$). Mortality gradually increased over the exposure hours at 40 °C. After 25 h of emersion, high mortality was observed (25 h, control: $n = 25$; transition: $n = 24$; vent: $n = 25$) (Fig. 8). At the end of each temperature treatment, greater mortality was observed in individuals exposed to 40 °C (98.7%) than in those exposed to 30 °C (34.7%).

Table 5
Results of the three-way permutational ANOVA analyzing desiccation tolerance with site (three levels: control, transition, vent), temperature (three levels: 20 °C, 30 °C, 40 °C) and hours of emersion (five levels: 5 h, 10 h, 15 h, 20 h, 25 h) as fixed factors. Results of *a posteriori* pairwise analysis for the interaction of factors temperature and hours of emersion ($p < 0.05$).

Desiccation tolerance						
Source of variation			*df*	MS	Pseudo-F	*p* (perm)
Site			2	0.17497	2.7137	0.0652
T °C			2	10.828	167.94	0.0002
Hours of emersion			4	1.4159	21.96	0.0002
Site x T °C			4	0.12468	1.9337	0.1107
Site x Hours of emersion			8	0.12504	1.9393	0.054
T °C x Hours of emersion			8	1.6518	25.619	0.0002
Site x T °C x Hours of emersion			16	8.3663E-2	1.2976	0.1872
Res			871	6.4476E-2		
Total			915			
Pairwise analyses						
Hours of emersion	20 °C		30 °C		40 °C	
	t	*p*	*t*	*p*	*t*	*p*
5 *vs* 10	0		3.2904	0.0015	2.9528	0.004
5 *vs* 15	0		0.87901	0.3734	7.2205	0.0002
5 *vs* 20	0		1.6367	0.1152	8.1388	0.0002
5 *vs* 25	0		0.85269	0.4369	10.738	0.0002
10 *vs* 15	0		2.2012	0.0272	3.7453	0.0005
10 *vs* 20	0		3.9178	0.0002	4.0267	0.0005
10 *vs* 25	0		3.4117	0.001	4.9336	0.0002
15 *vs* 20	0		2.267	0.0192	0.83188	0.4189
15 *vs* 25	0		1.5626	0.1282	2.2823	0.0252
20 *vs* 25	0		1.0881	0.3469	1.7265	0.093

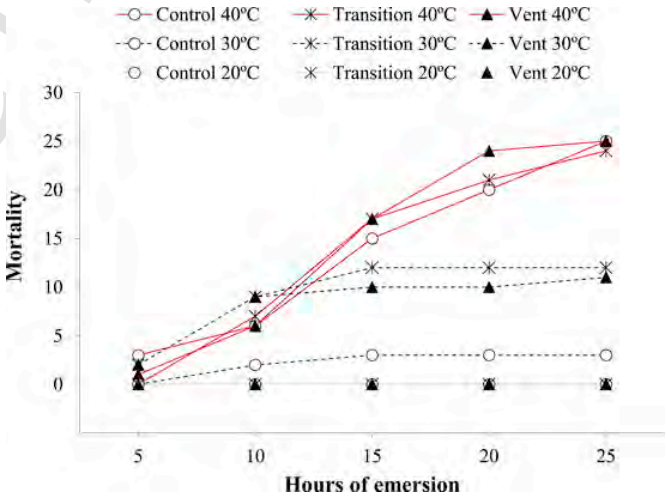

Fig. 8. Number of deaths of *P. sauciatus* individuals recorded during emersion hours (5–25 in 5 h increments) at each temperature treatment (20 °C, 30 °C, 40 °C). ($n = 25$ individuals *per* site for each T °C treatment).

4. Discussion

Volcanic CO_2 vents provide a unique possibility for the scientific community to explore individual and population responses to low pH environments (González-Delgado and Hernández, 2018). Temporal and rapid fluctuations in pH, carbonate saturation states, and alkalinity levels can occur at CO_2 vent sites due to coastal dynamics, changes in venting rate, or variations in biological processes (Kerrison et al., 2011). These changes in carbonate chemistry may be often more pronounced than those expected due to climate change during the twenty-first century (Rastrick et al., 2018).

Continuous data collection using autonomous sensors demonstrated that the volcanic CO_2 vent off La Palma Island creates natural pCO_2 and pH gradients along the shoreline (Hernández et al., 2017). No variability in the carbonate chemistry parameters was detected at the control site. In contrast, fluctuations in pH over tidal cycles were detected at the vent area, resulting in populations experiencing daily changes from ~8.15 to 7.00. Calcite and aragonite saturation states were also significantly reduced at the CO_2 vent. The lowest Ω calcite and Ω argonite values were found at the vent site during low tide. Moreover, the increased pCO_2 concentration was accompanied by large-scale changes in T_A between sites. A noticeable increase in T_A during low tide was detected at the vent site. T_A is a relatively conservative parameter, and such a strong variability has not been predicted to occur under OA conditions. While no filtration of groundwater was confirmed in the area by salinity measurements, it is possible that extensive dissolution of carbonate skeletons or the contribution of borates and mainly silicates could drive an increase in T_A. We are aware that the highly variable carbonate chemistry in the transition and vent sites is not representative of the future OA conditions; however, these sites do provide an excellent opportunity for studying the effects of variable pH on calcified marine invertebrates.

Previous studies at CO_2 vents in the Mediterranean have detected significant reductions in gastropod densities under acidified conditions (Hall-Spencer et al., 2008; Kroeker et al., 2011). In contrast, we found no effects of high pCO_2 on the population parameters. Our results showed no significant differences on population density or size-frequency distributions between control, transition, and vent sites. This finding suggests that *P. sauciatus* is able to maintain the population performance in a highly variable pH environment. Similarly, Fabricius et al. (2014) also observed no significant changes in total densities of molluscs at a shallow CO_2 vent in Papua New Guinea. Particularly, Connell et al. (2017) demonstrated that indirect effects of high pCO_2 did drive a greater abundance of an herbivore gastropod at a CO_2 vent in the southwest Pacific. However, the influence of these indirect effects on *P. sauciatus* population performance can only be speculative since were not explored in the present study. It is important to note that natural vents are open systems in which larvae from nearby populations can successfully settle and influence population density (Kroeker et al., 2011). *P. sauciatus* has external fertilization and recruits via planktonic larval dispersal (trochophore and veliger larvae) (Sousa et al., 2017), which might promote population connectivity. This connectivity could explain why no significant changes in population parameters were observed across the natural pH gradient.

We detected significant differences in shell shape (shell length:shell width) between individuals from the control and vent sites. Shells from the vent site exhibited a higher aspect ratio than those from the control site. The majority of studies on gastropods have reported that shell morphology and size were negatively impacted by elevated pCO_2 (*Littorina littorea*: Melatunan et al., 2013; *Anachis misera*: Chen et al., 2015; *Nassarius corniculus and Cyclope neritea*: Garilli et al., 2015; *Hexaplex trunculus*: Harvey et al., 2016; *Nucella lapillus*: Rühl et al., 2017; *Charonia lampas*: Harvey et al., 2018). However, these changes in shell features in response to changes in seawater chemistry are species-specific (Langer et al., 2014; Harvey et al., 2016). For example, Duquette et al. (2017) found that the shell length of top-shells snails (*Osilinus turbinatus*) decreased with reduced pH at a CO_2 vent area. In contrast, our results provide evidence of change in shell shape of *P. sauciatus* at the vent site, but shell length did not decrease with a reduction in pH. Indeed, on average, individuals from the vent site were taller than those from the control site. Preston and Roberts (2007) suggested that differences in shell morphology in intertidal gastropods are the result of rapid shell growth in response to environmental stressors, which results in larger and more elongated but not thicker shells. Moreover, elongated shell shapes might increase the risk of dislodgement by wave force (Trussell, 1997) or lead to changes in the species interactions (Xu et al., 2017). Future investigations are required to improve our understanding of the implications of these changes in shell shape at the community level.

Significant differences in the percentages of shell corrosion and break of individuals were observed between the control site with respect to the transition and vent sites. In contrast, shell conditions of individuals did not differ significantly between vent and transition sites. We found that shells from high pCO_2 sites exhibited greater percentages of dissolution and presence of holes or apex truncation than those at the control site. Evidence of shell deterioration in response to changes in seawater chemistry has been reported for other gastropods at CO_2 vents (Hall-Spencer et al., 2008; Milazzo et al., 2014; Chen et al., 2015; Garilli et al., 2015; Duquette et al., 2017; Harvey et al., 2018). Marine molluscs appear to have no control over shell dissolution (Nienhuis et al., 2010), a process that depends on the solubility, composition, and microstructure of the calcium carbonate biominerals (Hahn et al., 2012). The shell microstructure of the genus *Phorcus*, which is constituted by an organic periostracum coating, an outer prismatic and foliated calcitic layer, and an inner aragonitic layer, is dependent on the environmental parameters (García-Escárzaga et al., 2015). Our results provide evidence that pH fluctuations can significantly affect the shell integrity of *P. sauciatus*. Moreover, we interpret that the dissolution observed at the external surface of shells may be due to loss of the protective organic layer (Rodolfo-Metalpa et al., 2011) caused by carbonate chemistry changes over tidal cycles at the CO_2 vent area.

Some mollusc species are capable of counteracting shell dissolution by enhancing calcium carbonate production (Nienhuis et al., 2010; Findlay et al., 2011; Garilli et al., 2015). For example, Langer et al. (2014) observed that the addition of aragonitic layers increased in patellogastropod shells, while calcitic layers were confined to elongation growth but did not counteract shell dissolution. However, several studies reported that new shell material precipitated under lower pH conditions resulted in altered shell microstructure with irregular and disordered calcite and aragonite crystals, which could lead to loss of shell mechanical strength (Hahn et al., 2012; Wolfe et al., 2012; Duquette et al., 2017). In the present study, we found that fracture resistance differed significantly between study sites and shell sizes. The mean force needed to fracture shells from the control site differed significantly between all shell sizes and increased with shell width. In contrast, no significant differences in the fracture resistance was observed between small and medium-sized shells from the transition site. These sizes fractured in a similar force range and were, on average, less resistant than large-sized shells. No significant differences in the fracture resistance were observed between any of the sizes of shells from the vent site. We interpret that these changes in shell mechanical strength of *P. sauciatus* could be directly related to the dissolution of external surfaces observed but could also be indicative of inner shell dissolution (Melzner et al., 2011), allowing organisms to maintain their homeostasis under reduced pH values (Michaelidis et al., 2005). While shell thickness and shell mineralogy were not investigated in this study,

it is also possible that reductions in shell density and alterations in shell microstructure are responsible for weakened shells, as previously reported for other gastropod and bivalve species (Gaylord et al., 2011; Coleman et al., 2014; Langer et al., 2014; Harvey et al., 2018). Changes in shell shape can also impair the mechanical functions of the shell as primary defence against predation (Preston and Roberts, 2007; Harvey et al., 2018). The findings presented here are particularly relevant for *P. sauciatus* ecology. Reductions in shell strength could decrease the amount of energy required for crushing predators to breaking large-sized shells (Kroeker et al., 2014). Therefore, future research on this species should explore the influence of these changes in shell features on predator-prey interactions.

We found no significant differences in the desiccation tolerance between individuals from each study site, but significant differences between temperature and hours of emersion were detected. Previous studies have evidenced the influence of elevated *p*CO2 and warming on the metabolism of intertidal organisms such as barnacles, limpets and top-shell snails (Findlay et al., 2010; Legrand et al., 2018). Zhang et al. (2014) found that the interactive effects of pCO_2 and temperature increased larval mortality of an intertidal snail (*Nassarius festivus*). Furthermore, it has been suggested that elongated shell shapes can result in individuals more prone to water loss during emersion periods (Melatunan et al., 2013). Thus, in our study, higher mortality of individuals from high pCO_2 sites were expected to occur. Contrary to our expectations, our results showed no effect of reduced pH on desiccation tolerance of *P. sauciatus*. Mortality of individuals was mostly influenced by the cumulative hours of exposure at increased temperatures. Individuals exhibited greater tolerance at 20 °C and no mortality was observed at this temperature. At 30 °C, individuals exhibited lower tolerance and mortality increases until 15 h of exposure. Individuals suffered higher mortality at 40 °C, which gradually increased over the emersion hours. Most of the individual died after 25 h of exposure at this temperature. Our results agree with other studies, which have reported a decline in intertidal gastropod survival due to heat stress at temperatures >30 °C (Menzies et al., 1992; Miller et al., 2009; Gleason and Burton, 2013). Intertidal gastropods are exposed to larger daily and seasonal fluctuations in environmental conditions (such as temperature, oxygen, pH, salinity) (Sousa et al., 2017). The thermal physiology of these organisms plays a key role modulating their capability of coping with thermal stress coupled with aerial exposure and defining their intertidal position on rocky shores (Stickle et al., 2017; Drake et al., 2017). *P. sauciatus* survival in this experiment was more affected by elevated temperatures than elevated pCO_2. This result should be considered in terms of global warming. Intertidal rocky shore species live close to their physiological thermal limits; consequently, global temperature elevations and extreme heat waves could have a significant impact on their metabolism and survival (Tomanek, 2010; Burrows, 2017).

5. Conclusions

The present study investigated the effects of long-term exposure to reduced pH on the shells and survival of an intertidal gastropod in a volcanic CO_2 vent. Comparative studies of the population parameters, shell features, and desiccation tolerances were conducted between *P. sauciatus* populations across a natural pH gradient. By comparing population density and size-frequency, we found that *P. sauciatus* was capable of maintaining the population performance in a highly variable pH environment. In addition, we found similar desiccation tolerance among contrasting environment populations. We found no effects of high pCO_2 on resistance to desiccation, but *P. sauciatus* survival was negatively impacted by temperatures >30 °C during the experimental emersion periods. Future research is essential in order to better understand the responses of intertidal organisms to projected changes in temperature (Drake et al., 2017). Comparative studies of shell shapes and conditions showed that a reduction in pH values caused changes in shell shapes and shell dissolution. Moreover, reductions in shell fracture resistance were detected. Our results add to the growing body of evidence in which reduced pH and altered seawater chemistry have been shown to have a negative impact on shell morphology and integrity of marine gastropods. Loss of shell properties could have the potential to alter the species interaction and structure of intertidal communities (Kroeker et al., 2014). Therefore, we suggest that future investigations on this species should focus on the implications of these changes in shell features on ecological process and include long-term monitoring of population dynamics.

Uncited References

Fabricius et al., 2011, Hernández et al., 2015, Sousa et al., 2018

Acknowledgements

We thank B. Alfonso, S. González-Delgado and L. Epherra who helped during the sampling. We also extend our gratitude to K. Theofilis for assistance with digital image processing. We thank L. Hernández-Gutiérrez and M. González-Morales (Servicio de Laboratorios y Calidad de la Construcción, Gobierno de Canarias) for their assistance with crushing resistance measurements performed. This manuscript was written within the framework of the project Plan Nacional de Investigación of the Spanish Ministerio de Economía y Competitividad, BLUEROCK, CGL17 2013-43908-R and the support of the Fundación Biodiversidad, Ministerio para la Transición Ecológica. Finally, we thank Cabildo de La Palma for also supported this study and Ayuntamiento de Fuencaliente for the logistical collaboration.

References

Agostini, S., Harvey, B.P., Wada, S., Kon, K., Milazzo, M., Inaba, K., Hall-Spencer, J.M., 2018. Ocean acidification drives community shifts towards simplified non-calcified habitats in a subtropical–temperate transition zone. Sci. Rep. 8, 11354. Available from: https://doi.org/10.1038/s41598-018-29251-7.

Alfonso, B., Sarabia, A., Sancibrián, I., Alfaro, A., Adern, N., Hernández, J.C., 2015. Efecto de la actividad humana sobre la distribución y estructura poblacional del burgado Phorcus sauciatus (Koch, 1845). Rev. Acad. Canar. Cienc. 27, 333–343.

AnalystSoft Inc, 2013. StatPlus 5.4, AnalystSoft Inc., Alexandria, VA.

Anderson, M.J., 2001. Permutation tests for univariate or multivariate analysis of variance and regression. Can. J. Fish. Aquat. Sci. 58, 626–639. Available from: https://doi.org/10.1139/cjfas-58-3-626.

Anderson, M., Gorley, R.N., Clarke, R.K., 2008. PERMANOVA + for PRIMER: Guide to Software and Statistical Methods, PRIMER-E, Plymouth, UK. Available from: https://www.primer-e.com/.

Burrows, M.T., 2017. Intertidal species and habitats. MCCIP Sci. Rev. 62–72. Available from: https://dx.doi.org/10.14465/2017.arc10.006-ish 2017.

Carracedo, J.C., Rodríguez-Badiola, E., Guillou, H., Nuez, J., Pérez-Torrado, F.J., 2001. Geology and volcanology of La Palma and El hierro, western canaries. Estud. Geol. 57, 5–6. Available from: https://dx.doi.org/10.1016/0377-0273(94)90053-1.

Chen, Y.J., Wu, J.Y., Chen, C.T.A., Liu, L.L., 2015. Effects of low-pH stress on shell traits of the dove snail, Anachis misera. Biogeosciences 12, 2631–2639. Available from: https://dx.doi.org/10.5194/bg-12-2631-2015.

Coleman, D.W., Byrne, M., Davis, R.A., 2014. Molluscs on acid: gastropod shell repair and strength in acidifying oceans. Mar. Ecol. Prog. Ser. 509, 203–211. Available from: https://doi.org/10.3354/meps10887.

Connell, S.D., Doubleday, Z.A., Hamlyn, S.B., Foster, N.R., Harley, C.D.G., Helmuth, B., Kelaher, B.P., Nagelkerken, I., Sarà, G., Russell, B.D., 2017. How ocean acidification can benefit calcifiers. Curr. Biol. 27, 95–96. Available from: https://dx.doi.org/10.1016/j.cub.2016.12.004.

Cotton, P.A., Rundle, S.D., Smith, K.E., 2004. Trait compensation in marine gastropods: shell shape, avoidance behavior, and susceptibility to predation. Ecology 85, 1581–1584. Available from: https://doi.org/10.1890/03-3104.

Dickson, A.G., 1990. Standard potential of the reaction: AgCl(s) + 12H2(g) = Ag(s) + HCl(aq), and the standard acidity constant of the ion HSO4− in synthetic sea water from 273.15 to 318.15 K. J. Chem. Thermodyn. 22, 113–127. Available from: https://doi.org/10.1016/0021-9614(90)90074-z.

Dickson, A.G., Sabine, C.L., Christian, J.R., 2007. Guide to best practices for ocean CO_2 measurements. PICES Special Publ. 3, 191.

Donald, K.M., Preston, J., Williams, S.T., Reid, D.G., Winter, D., Alvarez, R., Buge, B., Hawkins, S.J., Templado, J., Spencer, H.G., 2012. Phylogenetic relationships elucidate colonization patterns in the intertidal grazers osilinus philippi, 1847 and Phor-

cus risso, 1826 (Gastropoda: Trochidae) in the northeastern Atlantic Ocean and mediterranean sea. Mol. Phylogenetics Evol. 62 (1), 35–45. Available from: https://dx.doi.org/10.1016/j.ympev.2011.09.002.

Drake, M.J., Miller, N.A., Todgham, A.E., 2017. The role of stochastic thermal environments in modulating the thermal physiology of an intertidal limpet, *Lottia digitalis*. J. Exp. Biol. 220, 3072–3083. Available from: https://dx.doi.org/10.1242/jeb.159020.

Duquette, A., McClintock, J.B., Amsler, C.D., Pérez-Huerta, A., Milazzo, M., Hall-Spencer, J.M., 2017. Effects of ocean acidification on the shells of four Mediterranean gastropod species near a CO_2 seep. Mar. Pollut. Bull. 124 (2), 917–928. Available from: https://dx.doi.org/10.1016/j.marpolbul.2017.08.007.

Fabricius, K.E., De'ath, G., Noonan, S., Uthicke, S., 2014. Ecological effect of ocean acidification and habitat complexity on reef-associated macroinvertebrate communities. P. Roy. Soc. B. 281, 20132479. Available from: https://doi.org/10.1098/rspb.2013.2479.

Fabricius, K.E., Langdon, C., Uthicke, S., Humphrey, C., Noonan, S., De'ath, G., Okazaki, R., Muehllehner, N., Glas, M.S., Lough, J.M., 2011. Losers and winners in coral reefs acclimatized to elevated carbon dioxide concentrations. Nat. Clim. Chang. 1, 165–169. Available from: https://doi.org/10.1038/nclimate1122.

Findlay, H.S., Kendall, M.A., Spicer, J.I., Widdicombe, S., 2010. Post-larval development of two intertidal barnacles at elevated CO2 and temperature. Mar. Biol. 157, 725–735. Available from: https://doi.org/10.1007/s00227-009-1356-1.

Findlay, H.S., Wood, H.L., Kendall, M.A., Spicer, J.I., Twitchett, R.J., Widdicombe, S., 2011. Comparing the impact of high CO_2 on calcium carbonate structures in different marine organisms. Mar. Biol. Res. 7 (6), 565–575. Available from: https://doi.org/10.1080/17451000.2010.547200.

García-Escárzaga, A., Moncayo, S., Gutiérrez-Zugasti, I., Martín-Chivelet, J., González-Morales, R., Cáceres, J.O., 2015. Mg/Ca ratios measured by Laser Induced Breakdown Spectroscopy (LIBS): a new approach to decipher environmental conditions. J. Anal. At. Spectrom. 30, 1913–1919. Available from: https://doi.org/10.1039/C5JA00168D.

Garilli, V., Rodolfo-Metalpa, R., Scuderi, D., Brusca, L., Parrinello, D., Rastrick, S.P.S., Foggo, A., Twitchett, R.J., Hall-Spencer, J.M., Milazzo, M., 2015. Physiological advantages of dwarfing in surviving extinctions in high–CO_2 oceans. Nat. Clim. Chang. 5, 678–682. Available from: https://doi.org/10.1038/nclimate2616.

Garrity, S.D., 1984. Some adaptations of gastropods to physical stress on a tropical rocky shore. Ecology 65 (2), 559–574. Available from: https://doi.org/10.2307/1941418.

Gaylord, B., Hill, T.M., Sanford, E., Lenz, E.A., Jacobs, L.A., Sato, K.N., Russell, A.D., Hettinger, A., 2011. Functional impacts of ocean acidification in an ecologically critical foundation species. J. Exp. Biol. 214, 2586–2594. Available from: https://doi.org/10.1242/jeb.055939.

Gazeau, F., Parker, L.M., Comeau, S., Gattuso, J.P., O'Connor, W.A., Martin, S., Pörtner, H.O., Ross, P.M., 2013. Impacts of ocean acidification on marine shelled molluscs. Mar. Biol. 160 (8), 2207–2245. Available from: https://doi.org/10.1007/s00227-013-2219-3.

Gleason, L.U., Burton, R.S., 2013. Phenotypic evidence for local adaptation to heat stress in the marine snail Chlorostoma (formerly Tegula) funebralis. J. Exp. Mar. Biol. Ecol. 448, 360–366. Available from: https://doi.org/10.1016/j.jembe.2013.08.008.

González-Delgado, S., Hernández, J.C., 2018. The importance of natural acidified systems in the study of ocean acidification: what have we learned? Adv. Mar. Biol. 80, 57–99. Available from: https://dx.doi.org/10.1016/bs.amb.2018.08.001.

Hahn, S., Rodolfo-Metalpa, R., Griesshaber, E., Schmahl, W.W., Buhl, D., Hall-Spencer, J., Baggini, C., Fehr, K., Immenhauser, A., 2012. Marine bivalve shell geochemistry and ultrastructure from modern low pH environments: environmental effect versus experimental bias. Biogeosciences 9, 1897–1914. Available from: https://dx.doi.org/10.5194/bg-9-1897-2012.

Hall-Spencer, J.M., Rodolfo-Metalpa, R., Martin, S., Ransome, E., Fine, M., Turner, S.M., Rowley, S.J., Tedesco, D., Buia, M.C., 2008. Volcanic carbon dioxide vents show ecosystem effects of ocean acidification. Nature 454, 96–99. Available from: https://doi.org/10.1038/nature07051.

Harvey, B.P., Gwynn-Jones, D., Moore, P.J., 2013. Meta-analysis reveals complex marine biological responses to the interactive effects of ocean acidification and warming. Ecol. Evol. 3 (4), 1016–1030. Available from: https://doi.org/10.1002/ece3.516.

Harvey, B.P., McKeown, N.J., Rastrick, P.S., Bertolini, C., Foggo, A., Graham, H., Hall-Spencer, J.M., Milazzo, M., Shaw, P.W., Small, D.P., Moore, P.J., 2016. Individual and population-level responses to ocean acidification. Sci. Rep. 4. Available from: https://doi.org/10.1038/srep20194 20194.

Harvey, B.P., Agostini, S., Wada, S., Inaba, K., Hall-Spencer, J.M., 2018. Dissolution: the achilles' heel of the triton shell in an acidifying ocean. Front. Mar. Sci. 5, 371. Available from: https://doi.org/10.3389/fmars.2018.00371.

Hernández, C.A., Clemente, S., Sangil, C., Hernández, J.C., 2015. High-resolution ocean pH dynamics in four subtropical Atlantic benthic habitats. Biogeosci. Discuss. 12, 19481–19498. Available from: https://doi.org/10.5194/bgd-12-19481-2015.

Hernández, J.C., Sangil, C., Hernández, C.A., Epherra, L., González-Delgado, S., Viotti, S., Alfonso, B., Pérez-Álvarez, C., 2017. Exploración de las surgencias submarinas de CO_2 en las costas de Fuencaliente. Technical Report, University of La Laguna, p. 58.

IPCC, 2014. In: Pachauri, R.K., Meyer, L.A. (Eds.), Core Writing Team. In: Climate Change 2014: Synthesis Report. Contribution of Working Groups I, II and III to the Fifth Assessment Report of the Intergovernmental Panel on Climate Change, p. 151 Geneva (Switzerland).

Kerrison, P., Hall-Spencer, J.M., Suggett, D.J., Hepburn, L.J., Steinke, M., 2011. Assessment of pH variability at a coastal CO2 vent for ocean acidification studies. Estuar. Coast Shelf Sci. 94 (2), 129–137. Available from: https://dx.doi.org/10.1016/j.ecss.2011.05.025.

Kroeker, K.J., Kordas, R.L., Crim, R., Hendriks, I.E., Ramajo, L., Singh, G.S., Duarte, C.M., Gattuso, J.P., 2013. Impacts of ocean acidification on marine organisms quantifying sensitivities and interaction with warming. Glob. Chang. Biol. 19, 1884–1896. Available from: https://doi.org/10.1111/gcb.12179.

Kroeker, K.J., Micheli, F., Gambi, M.C., Martz, T.R., 2011. Divergent ecosystem responses within a benthic marine community to ocean acidification. P. Natl. Acad. Sci. USA. 108, 14515–14520. Available from: https://doi.org/10.1073/pnas.1107789108.

Kroeker, K.J., Sanford, E., Jellison, B.M., Gaylord, B., 2014. Predicting the effects of ocean acidification on predator-prey interactions: a conceptual framework based on coastal molluscs. Biol. Bull. 226 (3), 211–222. Available from: https://doi.org/10.1086/BBLv226n3p211.

Kurihara, H., 2008. Effects of CO_2-driven ocean acidification on the early developmental stages of invertebrates. Mar. Ecol. Prog. Ser. 373, 275–284. Available from: https://doi.org/10.3354/ab00109.

Langer, G., Nehrke, G., Baggini, C., Rodolfo-Metalpa, R., Hall-Spencer, J.M., Bijma, J., 2014. Limpets counteract ocean acidification induced shell corrosion by thickening of aragonitic shell layers. Biogeosciences 11, 7363–7368. Available from: https://doi.org/10.5194/bg-11-7363-2014.

Langer, G., Sadekov, A., Nehrke, G., Baggini, C., Rodolfo-Metalpa, R., Hall-Spencer, J.M., Cuoco, E., Bijma, J., Elderfield, H., 2018. Relationship between mineralogy and minor element partitioning in limpets from the Ischia CO2 vent site provides new insights into their biomineralization pathway. Geochem. Cosmochim. Acta 236, 218–229. Available from: https://doi.org/10.1016/j.gca.2018.02.044.

Legrand, E., Riera, P., Bohner, O., Coudret, J., Schlicklin, F., Derrien, M., Martin, S., 2018. Impact of ocean acidification and warming on the productivity of a rock pool community. Mar. Environ. Res. 136, 78–88. Available from: https://doi.org/10.1016/j.marenvres.2018.02.010.

Lewis, E., Wallace, D.W.R., 1998. Program Developed for CO2 System Calculations, ORNL/CDIAC-105, Carbon Dioxide Inf. Anal. Cent., Oak Ridge Natl. Lab., Oak Ridge, Tenn., p. 38.

McClintock, J.B., Angus, R.A., McDonald, M.R., Amsler, C.D., Catledge, S.A., Vohra, Y.K., 2009. Rapid dissolution of shells of weakly calcified Antarctic benthic macroorganisms indicates high vulnerability to ocean acidification. Antarct. Sci. 21, 449–456. Available from: https://doi.org/10.1017/S0954102009990198.

Melatunan, S., Calosi, P., Rundle, S.D., Widdicombe, S., Moody, A.J., 2013. Effects of ocean acidification and elevated temperature in shell plasticity and its energetic basis in an intertidal gastropod. Mar. Ecol. Prog. Ser. 472, 155–168. Available from: https://doi.org/10.3354/meps10046.

Menzies, R., Cohen, Y., Lavie, B., Nevo, E., 1992. Niche adaptation in two marine gastropods, Monodonta turbiformis and M. turbinata. Boll. di zool. 59 (3), 297–302. Available from: https://doi.org/10.1080/11250009209386685.

Mehrbach, C., Culberson, C.H., Hawley, J.E., Pytkowicz, R.M., 1973. Measurement of the apparent dissociation constants of carbonic acid in seawater at atmospheric pressure. Limnol. Oceanogr. 18, 897–907. Available from: https://doi.org/10.4319/lo.1973.18.6.0897.

Melzner, F., Stange, P., Trübenbach, K., Thomsen, J., Casties, I., Panknin, U., Gorb, S., Gutowska, M.A., 2011. Food supply and seawater pCO_2 impact calcification and in-

ternal shell dissolution in the blue mussel Mytilus edulis. PLoS One 6. Available from: https://doi.org/10.1371/journal.pone.0024223, e24223.
Meng, Y., Guo, Z., Fitzer, S.C., Upadhyay, A., Chan, V.B.S., Li, C., Cusack, M., Yao, H., Yeung, K.W.K., Thiyagarajan, V., 2018. Ocean acidification reduces hardness and stiffness of the Portuguese oyster shell with impaired microstructure: a hierarchical analysis. Biogeosciences 15, 6833–6846. Available from: https://dx.doi.org/10.5194/bg-15-6833-2018.
Michaelidis, B., Ouzounis, C., Paleras, A., Portner, H.O., 2005. Effects of long-term moderate hypercapnia on acid–base balance and growth rate in marine mussels Mytilus galloprovincialis. Mar. Ecol. Prog. Ser. 293, 109–118. Available from: https://doi.org/10.3354/meps293109.
Milazzo, M., Alessi, C., Quattrocchi, F., Chemello, R., D'Agostaro, R., Gil, J., Vaccaro, A.M., Mirto, S., Gristina, M., Badalamenti, F., 2019. Biogenic habitat shifts under long-term ocean acidification show nonlinear community responses and unbalanced functions of associated invertebrates. Sci. Total Environ. 667, 41–48. Available from: https://doi.org/10.1016/j.scitotenv.2019.02.391.
Milazzo, M., Rodolfo-Metalpa, R., San-Chan, V.B., Fine, M., Alessi, C., Thiyagarajan, V., Hall-Spencer, J.M., Chemello, R., 2014. Ocean acidification impairs vermetid reef recruitment. Sci. Rep. 4, 4189. Available from: https://dx.doi.org/10.1038/srep04189.
Miller, L.P., Harley, C.D., Denny, M.W., 2009. The role of temperature and desiccation stress in limiting the local-scale distribution of the owl limpet, Lottia gigantea. Funct. Ecol. 23, 756–767. Available from: https://doi.org/10.1111/j.1365-2435.2009.01567.x.
Nienhuis, S., Palmer, A.R., Harley, C.D.G., 2010. Elevated CO_2 affects shell dissolution rate but not calcification rate in a marine snail. P. Roy. Soc. B. 277, 2553–2558. Available from: https://doi.org/10.1098/rspb.2010.0206.
Onitsuka, T., Kimura, R., Ono, T., Takami, H., Nojiri, Y., 2014. Effects of ocean acidification on the early developmental stages of the horned turban, Turbo cornutus. Mar. Biol. 161, 1127–1138. Available from: https://doi.org/10.1007/s00227-014-2405-y.
Padrón, E., Pérez, N.M., Rodríguez, F., Melián, G., Hernández, P.A., Sumino, H., Padilla, G., Barrancos, J., Dionis, S., Notsu, K., Calvo, D., 2015. Dynamics of carbon dioxide emissions from Cumbre Vieja volcano, La Palma, canary islands. Bull. Volcanol. 77, 28. Available from: https://doi.org/10.1007/s00445-015-0914-2.
Pörtner, H.O., 2008. Ecosystem effects of ocean acidification in times of ocean warming: a physiologist's view. Mar. Ecol. Prog. Ser. 373, 20–217. Available from: https://doi.org/10.3354/meps07768.
Preston, S.J., Roberts, D., 2007. Variation in shell morphology of calliostoma zizyphinum (Gastropoda Trochidae). J. Molluscan Stud. 73, 101–104. Available from: https://doi.org/10.1093/mollus/eyl034.
R Development Core Team, 2016. R: A Language and Environment for Statistical Computing, R Foundation for Statistical Computing, Vienna, Austria.
Rastrick, S.S.P., Graham, H., Azetsu-Scott, K., Calosi, P., Chierici, M., Fransson, A., Hop, H., Hall-Spencer, J., Milazzo, M., Thor, P., Kutti, T., 2018. Using natural analogues to investigate the effects of climate change and ocean acidification on Northern ecosystems. ICES J. Mar. Sci.. Available from: https://dx.doi.org/10.1093/icesjms/fsy128.
Ries, J.B., Cohen, A.L., McCorkle, D.C., 2009. Marine calcifiers exhibit mixed responses to CO_2-induced ocean acidification. Geology 37, 1131–1134. Available from: https://dx.doi.org/10.1130/G30210A.1.
Rodolfo-Metalpa, R., Houlbreque, F., Tambutte, E., Boisson, F., Baggini, C., Patti, F.P., Jeffree, R., Fine, M., Foggo, A., Gattuso, J.P., Hall-Spencer, J.M., 2011. Coral and mollusc resistance to ocean acidification adversely affected by warming. Nat. Clim. Chang. 1, 308–312. Available from: https://doi.org/10.1038/nclimate1200.
Rühl, S., Calosi, P., Faulwetter, S., Keklikoglou, K., Widdicombe, S., Queiros, A.M., 2017. Long-term exposure to elevated pCO_2 more than warming modifies early-life shell growth in temperate gastropod. ICES J. Mar. Sci. 74 (4), 1113–1124. Available from: https://doi.org/10.1093/icesjms/fsw242.
Schneider, C.A., Rasband, W.S., Eliceiri, K.W., 2012. NIH Image to ImageJ: 25 years of image analysis. Nat. Methods 9 (7), 671–675. Available from: https://doi.org/10.1038/nmeth.2089.
Sousa, R., Delgado, J., González, J.A., Freitas, M., Henriques, P., 2017. Marine Snails of the Genus Phorcus: Biology and Ecology of Sentinel Species for Human Impacts on the Rocky Shores. Biological Resources of Water. Available from: https://doi.org/10.5772/intechopen.71614 Sajal Ray, IntechOpen.
Sousa, R., Vasconcelos, J., Delgado, J., Riera, R., González, J.A., Freitas, M., Henriques, P., 2018. Filling biological information gaps of the marine topshell Phorcus sauciatus (Gastropoda: Trochidae) to ensure its sustainable exploitation. J. Mar. Biol. Assoc. U. K. 1–9. Available from: https://dx.doi.org/10.1017/S0025315418001054.
Stephenson, T.A., Stephenson, A., 1949. The universal features of zonation between tide-marks on rocky coasts. J. Ecol. 37, 289–305. Available from: https://doi.org/10.2307/2256610.
Stickle, B.W., Carrington, E., Hayford, H., 2017. Seasonal changes in the thermal regime and gastropod tolerance to temperature and desiccation stress in the rocky intertidal zone. J. Exp. Mar. Biol. Ecol. 488, 83–91. Available from: https://dx.doi.org/10.1016/j.jembe.2016.12.006.
Sunday, J.M., Calosi, P., Dupont, S., Munday, P.L., Stillman, J.H., Reusch, T.B., 2014. Evolution in an acidifying ocean. Trends Ecol. Evol. 29, 117–125. Available from: https://doi.org/10.1016/j.tree.2013.11.001.
Tomanek, L., 2010. Variation in the heat shock response and its implication for predicting the effect of global climate change on species biogeographic distribution ranges and metabolic costs. J. Exp. Biol. 213, 971–979. Available from: https://doi.org/10.1242/jeb.038034.
Trussell, G.C., 1997. Phenotypic plasticity in the foot size of an intertidal snail. Ecology 78 (4), 1033–1048. Available from: https://doi.org/10.1890/0012-9658(1997)078[1033:PPITFS]2.0.CO;2.
Uppström, L.R., 1974. The boron/chlorinity ratio of deep-seawater from the Pacific Ocean. Deep-Sea Res. 21, 161–162. Available from: https://dx.doi.org/10.1016/0011-7471(74)90074-6.
Uribe, J.E., Williams, S.T., Templado, J., Buge, B., Zardoya, R., 2017. Phylogenetic relationships of mediterranean and north-east atlantic cantharidinae and notes on stomatellinae (vetigastropoda: Trochidae). Mol. Phylogenetics Evol. 107, 64–79. Available from: https://doi.org/10.1016/j.ympev.2016.10.009.
Vermeij, G.J., 1973. Morphological patterns in high-intertidal gastropods: adaptive strategies and their limitations. Mar. Biol. 20, 319–346. Available from: https://dx.doi.org/10.1007/BF00354275.
Wolfe, K., Smith, A.M., Trimby, P., Byrne, M., 2012. Vulnerability of the paper nautilus (Argonauta nodosa) shell to a climate-change ocean: potential for extinction by dissolution. Biol. Bull. 223 (2), 236–244. Available from: https://doi.org/10.1007/s00227-012-2032-4.
Xu, X.-Y., Yip, K.R., Shin, P.K.S., Cheung, S.G., 2017. Predator–prey interaction between muricid gastropods and mussels under ocean acidification. Mar. Pollut. Bull. 124 (2), 911–916. Available from: https://dx.doi.org/10.1016/j.marpolbul.2017.01.003.
Zhang, H., Cheung, S.G., Shin, K.S.P., 2014. The larvae of congeneric gastropods showed differential responses to the combined effects of ocean acidification, temperature and salinity. Mar. Pollut. Bull. 79 (1–2), 39–46. Available from: https://dx.doi.org/10.1016/j.marpolbul.2014.01.008.